

AD-A068 681

NAVAL RESEARCH LAB WASHINGTON D C
NUCLEAR TECHNIQUES FOR PLASMA DIAGNOSTICS. (U)
APR 79 F C YOUNG
NRL-MR-3987

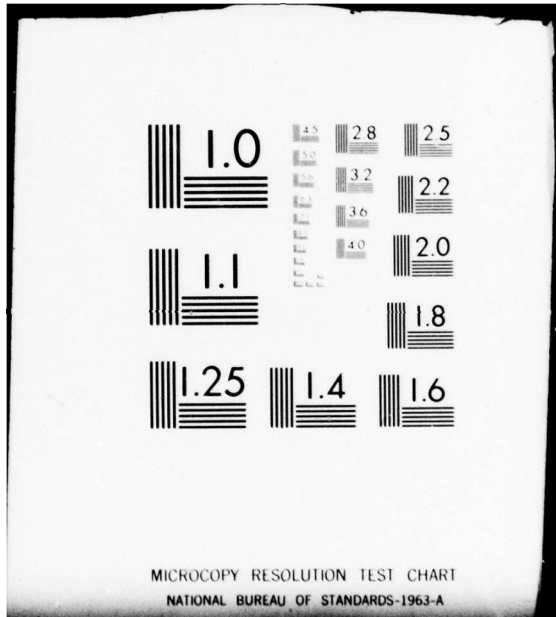
F/G 20/9

UNCLASSIFIED

NL

1 OF 1
AD
A068681





MICROCOPY RESOLUTION TEST CHART
NATIONAL BUREAU OF STANDARDS-1963-A

LEVEL

NRL Memorandum Report 3987

12

Nuclear Techniques for Plasma Diagnostics

FRANK C. YOUNG

Plasma Physics Division

April 23, 1979

DDC
RECEIVED
MAY 17 1979
D

This Research was sponsored in part by the Defense Nuclear Agency under subtask T99QAXLA014, work unit 46 and work unit title Ion Beam Generation.



79 05 16 003

NAVAL RESEARCH LABORATORY
Washington, D.C.

Approved for public release; distribution unlimited.

AD A068681

DDC FILE COPY

UNCLASSIFIED

SECURITY CLASSIFICATION OF THIS PAGE (When Data Entered)

9 REPORT DOCUMENTATION PAGE		READ INSTRUCTIONS BEFORE COMPLETING FORM
1. REPORT NUMBER NRL Memorandum Report 3987	2. GOVT ACCESSION NO.	3. RECIPIENT'S CATALOG NUMBER
4. TITLE (and Subtitle) NUCLEAR TECHNIQUES FOR PLASMA DIAGNOSTICS	5. TYPE OF REPORT & PERIOD COVERED Interim report on a continuing NRL problem.	
7. AUTHOR(s) Frank C. Young	6. CONTRACT OR GRANT NUMBER(s)	
9. PERFORMING ORGANIZATION NAME AND ADDRESS Naval Research Laboratory Washington, DC 20375	10. PROGRAM ELEMENT, PROJECT, TASK AREA & WORK UNIT NUMBERS NRL Problem H02-26A and H02-29A DNA Subtask T99QAXLA014	
11. CONTROLLING OFFICE NAME AND ADDRESS Defense Nuclear Agency, Washington, DC 20305 and Department of Energy, Washington, DC 20545	12. REPORT DATE April 1979	13. NUMBER OF PAGES 42
14. MONITORING AGENCY NAME & ADDRESS (if different from Controlling Office) 1242p.	15. SECURITY CLASS. (of this report) UNCLASSIFIED	
16. DISTRIBUTION STATEMENT (of this Report) Approved for public release; distribution unlimited. 14 NRL-MR-3987		
17. DISTRIBUTION STATEMENT (of the abstract entered in Block 20, if different from Report) 16 T99QAXL 17 A014		
18. SUPPLEMENTARY NOTES This research was sponsored in part by the Defense Nuclear Agency under subtask T99QAXLA014, work unit 46 and work unit title Ion Beam Generation. This report contains the text of a lecture presented at the 1978 IEEE Minicourse on Modern Plasma Diagnostics, Monterey, CA, May 1978.		
19. KEY WORDS (Continue on reverse side if necessary and identify by block number) High power pulsed plasmas Nuclear activations with intense ion beams Neutron activation detection Collective acceleration Neutron scintillation detection 100 10 to the 12th power		
20. ABSTRACT (Continue on reverse side if necessary and identify by block number) Recent developments of nuclear techniques to measure neutrons and positive ions emitted from pulsed-plasma devices are reviewed. Neutron detection for intensities ranging from 10^2 to 10^{12} neutrons/pulse is described. Activation detectors are useful for yields exceeding 10^9 neutrons. Scintillation detectors are required for less intense yields and for neutron measurements by time-of-flight. Intense pulsed ion beams are measured with nuclear reactions which produce delayed radioactivity. This activation technique is reviewed for proton, deuteron and alpha particle beams. 1,000,000		

DD FORM 1 JAN 73 1473

EDITION OF 1 NOV 65 IS OBSOLETE
S/N 0102-014-6601

UNCLASSIFIED

SECURITY CLASSIFICATION OF THIS PAGE (When Data Entered)

251 950

19

LB

TABLE OF CONTENTS

I.	ROLE OF NUCLEAR TECHNIQUES IN FUSION	1
II.	NEUTRON DETECTION	3
	Activation Detectors	3
	Scintillation Detectors	5
	Time-of-Flight Technique	7
III.	ION DETECTION	9
	Pulsed Ion Beams	9
	Collective Acceleration	13
IV.	APPENDIX	14

ACCESSION for		
DTIC	White Section	<input checked="" type="checkbox"/>
DDI	Staff Section	<input type="checkbox"/>
UNANNOUNCED		<input type="checkbox"/>
JUSTIFICATION		
BY		
DISTRIBUTION/AVAILABILITY CODES		
Dist.	AVAIL.	and/or SPECIAL
A		

NUCLEAR TECHNIQUES FOR PLASMA DIAGNOSTICS

I. ROLE OF NUCLEAR TECHNIQUES IN FUSION

Fusion is a nuclear process. Deuterium and tritium nuclei are fused by the $d(t,n)^4\text{He}$, $d(d,n)^3\text{He}$ and $d(d,p)t$ reactions to release energy. Both the d-t and d-d processes are characterized by the emission of MeV-type neutrons and ions (Fig. 1). The measurement of these radiations provides a direct indication that fusion reactions have taken place in a plasma. Techniques developed for studying nuclear reactions are amenable to characterizing these radiations from plasmas in the laboratory. In this talk I shall review some of the recent developments in this area as applied to pulsed-plasma devices. In most plasma devices neutrons are more readily measured than ions because neutrons can penetrate the plasma and containing walls or vacuum container to detectors located outside. For applications such as the development of intense ion beams and collective acceleration of ions, direct ion measurements are preferred. Most experimental studies have used the d-d reactions to avoid the problem of tritium radioactivity even though the d-d yield is about 10^2 smaller than the d-t yield at low energies.¹

One purpose for making measurements of neutrons from pulsed plasma sources is to determine the mechanism of neutron production. Therefore measurements, not only of the total neutron yield, but also the neutron energy, angular distribution and source location are desired. An important concern is the role of neutron production by low energy fusion reactions compared to neutron production by the acceleration of ions in a beam-target process. The latter process is likely to produce neutrons with different energies and angular distributions than that expected from a low energy fusion process. To evaluate such processes, precise angular distributions and energy determinations ($\leq 10\%$ uncertainty) may be required.

Note: Manuscript submitted March 1, 1979.

For a plasma confined and heated to fusion temperatures, neutron and ion measurements provide information about the energetics of the ions in a plasma. Energy is usually coupled to the plasma directly to the electrons, but the energy must be shared with the ions to achieve fusion. A measurement of the total number of neutrons produced by such a plasma indicates how much of the fuel in the plasma is consumed by fusion. Because the neutron yield is strongly dependent on the ion energy, such yields measure the magnitude of ion heating in a plasma. This is usually specified by an ion temperature; an average kinetic energy for the ion species. For a plasma containing N deuterons confined in a volume V , the rate of neutron production is given by

$$R = \frac{1}{2} N^2 \langle \sigma v \rangle / V$$

where $\langle \sigma v \rangle$ is the product of the fusion reaction cross section and the relative velocity of the deuterons averaged over the velocity distribution of the deuterons in the plasma. The quantity $\langle \sigma v \rangle$ is a sensitive function of ion temperature as indicated in Fig. 2 for a Maxwellian velocity distribution.¹ For any particular plasma source the scaling of neutron yield with ion temperature may involve a description of the energy coupling processes which leads to a non-Maxwellian ion velocity distribution. Even so, the neutron yield remains sensitively dependent on the ion energy. In fact, the scaling of neutron yield with energy coupled to the plasma may provide a test of our understanding of the energy-coupling processes. Because the neutron yield is so strongly dependent on the ion temperature, an uncertainty of a factor of 2 in the neutron yield provides a reasonably precise ion temperature determination.

II. NEUTRON DETECTION

What intensity of neutrons can be expected from a plasma? Let's start by asking how many reactions are necessary to produce 1 MJ of energy. For the $d(t,n)\alpha$ reaction, more than 10^{17} reactions are required, and a 1 MW power plant would require even more reactions. Present day plasmas are several orders of magnitude less than this level. The largest yields are of the order of 10^{12} neutrons from plasma-focus and exploded-wire devices which involve both thermal and non-thermal reactions. As break-even fusion is approached, neutron yields can be expected to increase dramatically. On the other hand, a small plasma device may produce less than 10^3 neutrons. For a source of less than 10^2 neutrons, the statistics on the number of events limits the usefulness of any measurement. In general, neutron detection ranging from 10^2 to greater than 10^{12} total neutrons is desired. A variety of detectors are required to encompass this large range of detection.

For a pulsed-plasma source, neutrons are usually emitted in a short burst in conjunction with an intense pulse of electromagnetic and x-ray radiation. The neutron detector must withstand this intense radiation pulse and measure the burst of neutrons. Two different types of detectors have been developed to make such measurements.

Activation Detectors

To avoid the x-ray flash, a detector which counts delayed radioactivity induced by neutrons is used. Delayed response counters which use Ag, Rh or Pb for neutron activation have been developed for such measurements on plasma sources. The limits of detectability and other properties of these detectors are summarized in Table 1. The limits given in this table correspond to a measured count of twice background for the counting time given. These detectors are generally useful for yields exceeding 10^6 to 10^7 neutrons. The counter may be surrounded with a neutron moderator to improve sensitivity, but this leads to practically

no discrimination against neutrons of different energies. Detailed descriptions of these counters may be found in the literature.²⁻⁵ A brief description of each counter is given here.

The Ag counter² consists of four Geiger tubes wrapped with Ag foils and embedded in a polyethylene moderator. The Geiger tubes measure the β -decay of Ag activated by moderated neutrons. This counter may have appreciable dead-time losses for intense bursts of neutrons because the Geiger tubes have an appreciable dead-time ($> 100 \mu\text{sec}$). In a study³ of this effect on one such counter dead-time losses were apparent (10% correction) for measured counts of $2 \times 10^4/60 \text{ sec}$ and the counter became unusable for measured counts exceeding $2 \times 10^5/60 \text{ sec}$.

The Rh-counter^{3,4} is less susceptible to dead-time losses because it uses a plastic scintillator, photomultiplier and commercial electronics capable of 10- μsec pulse-pair resolution. A schematic of this detector is given in Fig. 3. The Rh-foil is embedded in a polyethylene moderator. The scintillator measures the β -decay of Rh activated by moderated neutrons. The light pipe provides for moderation and backscatter of neutrons which pass through the foil. The Rh-counter is significantly smaller than the Ag counter and more useful for angular distribution measurements.

The Pb activation counter⁵ is sensitive to fast neutrons and does not use neutron moderation. A 5-inch dia. by 5-inch plastic scintillator totally encased in lead is used to measure the activation of $^{207\text{m}}\text{Pb}$ by neutrons with energies greater than a threshold of 1.6 MeV. The sensitivity of this counter increases by a factor of about 35 as the neutron energy increases from 2.5 to 14 MeV. Since the response of a moderated counter is relatively insensitive to variation in the neutron energy, a comparison of yields measured with the Pb-activation counter and a moderated counter can provide information about the neutron energy spectrum.

These detectors are usually calibrated with neutrons from radioactive sources or from a d-d or d-t generator. Such calibrations may not be applicable to measurements on a particular plasma device because neutron scattering and absorption may alter the calibration. To assess the importance of scattering and absorption, measurements with a radioactive source can be made with the detector in situ on the plasma device. Measurements of sources with different neutron energy spectra (e.g. Am-Be and ^{252}Cf) can be used to study the dependence of neutron scattering and absorption on neutron energy. See Ref. 3 for an application of this technique to a particular plasma device.

Scintillation Detectors

Scintillation counting of neutrons is required to measure neutron yields from less intense pulsed-plasma sources. To avoid the x-ray flash problem neutron interactions in the scintillator may be delayed by using a moderator. The most sensitive detection system uses a glass scintillator loaded with the isotope ^6Li and embedded in a polyethylene moderator. A schematic of such a detector is given in Fig. 4. Relatively large pulse-height signals arise from the $^6\text{Li}(n,\alpha)^3\text{H}$ reaction ($Q = 4.78$ MeV) in the scintillator. The cross section for this reaction is several barns for $E_n < 10$ keV. Moderated neutrons interact in the scintillator producing a standard pulse height for individual interactions. The moderator causes interactions in the scintillator to be delayed and dispersed in time up to several hundred microseconds after the neutron burst. A time spectrum corresponding to a single burst of neutrons is shown in Fig. 5. The initial pulse is the x-ray response which saturates the electronics. A pulse-height spectrum of the neutron events in this detector gives a resolution of about 30%. During an interval of about 300 μsec following the x-ray response, neutron interactions can be measured with essentially zero background. The sensitivity of this detector is such that, on the average, one interaction can be detected from a pulsed source of 75 neutrons total yield located

5 cm from the front face of the detector. Neutron yields ranging from 10^2 up to 10^7 can be measured with detectors of this type. A smaller detector with a 2-inch dia. scintillator can be used where less sensitivity is required.

To detect neutrons with an unmoderated scintillator, a time-of-flight path for the neutrons is required to separate their interaction in the scintillator from the x-ray flash. A fast recovery detector and a flight path of at least a meter are usually required for MeV neutrons. This naturally leads to a reduced sensitivity. Instead of using a flight path, one may try to eliminate the x-ray flash with high-Z shielding between the scintillator and plasma source. However, the neutron response in the scintillator is usually much smaller than the x-ray response so that a clean separation of these responses with shielding is difficult at best and not recommended.

Yield measurements with a fast-time response organic scintillator are complicated by nature of the neutron interaction in the scintillator. Neutrons interact in the scintillator primarily by n-p elastic scattering. For a neutron energy E_n , the proton recoil energy is given by $E_p = E_n \cos^2 \theta$ where θ is the proton scattering angle. The neutron may transfer any energy ranging from zero up to E_n to the recoiling proton. Consequently the detector response to a single neutron interaction ranges from zero to a maximum value proportional to the neutron energy. To determine the neutron yield for a burst of monoenergetic neutrons, the number of neutron interactions in the scintillator must be large enough so that the measured response represents a statistically significant average over the distribution of individual responses. This requires at least ~ 100 interactions in the detector. For a flight path of one meter and a 15 cm dia. detector, the source strength must be at least 10^5 neutrons. At this level, a ^6Li -glass scintillator detector can be used more straightforwardly for yield measurements.

Proportional counters such as BF_3 gas-filled counters embedded in a moderator are highly sensitive neutron detectors. However, such counters are limited for plasma applications because they have dead times of $\sim 100 \mu\text{sec}$.

Time-of-Flight Technique

The pulsed nature of many plasma sources makes the time-of-flight technique ideal for measuring neutron energies. The neutron energy is determined from a measurement of the neutron flight time for a known flight path. With fast scintillators and photomultipliers a time resolution of 5 to 10 nsec is achieved typically. A 2.45 MeV (14.1 MeV) neutron has a flight time of 46 ns/m (19 ns/m) so flight paths of several meters are usually used to separate the neutrons and x rays. In experiments where the x-ray pulse is sufficiently intense, techniques have been developed to gate off the photomultiplier during the initial x-ray burst and turn it on before the neutrons arrive at the detector.¹⁶

A time-of-flight measurement is illustrated in Fig. 6 for neutrons generated from a deuterium-loaded vacuum spark device. These traces were obtained with a 12-inch dia. scintillator coupled by a light pipe to a 5-inch dia. photomultiplier. The response time (FWHM) for this large detector was about 20 nsec. The neutron signal is well separated from the x rays at these flight paths. If the neutrons are emitted simultaneously with the x rays, a neutron energy of 2.5 ± 0.1 MeV is inferred. These neutron traces correspond to only 9 neutron interactions in the scintillator at 2.26 m and 4 interactions at 4.17 m based on yields obtained with a ^6Li -glass scintillator.⁴

As the flight path is increased, the recovery time required for a given neutron energy increases linearly, but the number of neutrons incident on a given detector decreases quadratically. Therefore a compromise must be made between detector sensitivity and highest measurable neutron energy in selecting a flight path.

The energy resolution is also determined by the flight path because the energy resolution is directly proportional to the time resolution ($\delta E/E = -2 \delta t/t$). As the flight path is increased, t increases, but the time resolution δt remains fixed so the energy resolution scales inversely with the flight path.

Let me illustrate the value of the time-of-flight technique by two extreme examples. If the neutron yield is sufficiently large so that very long flight paths can be used, then the time spread of the neutron response is dominated by the spread in energy of ions in the plasma rather than by the detector response time or the plasma duration. Under these circumstances, this technique has been used to determine the ion temperature in a laser-produced plasma experiment at Lawrence Livermore Laboratory.⁶ Neutron spectrometers with 3.5-ns time resolution are located 44.5 m from a plasma source which is produced with a 40 psec laser pulse. The time spread of the neutron response for 14 MeV neutrons is measured to determine ion temperatures of 5 to 6 keV for total yields of $\sim 5 \times 10^8$ neutrons.⁶

In the second example, the neutron flight path is sufficiently short, and the detector response time small enough so that the time spread of the neutron response is dominated by the duration of the pulsed plasma source. Under these circumstances, in experiments at NRL, the variation of the ion current with time of an intense pulsed deuteron beam has been determined by measuring the neutron response.⁷ Neutrons produced by an intense deuteron beam of ~ 0.7 MeV incident on a deuterated polyethylene target are measured with shielded detectors located ~ 2 meters from the target. The deuteron current in the diode is inferred from the duration and shape of the neutron response in the detector.⁷

III. ION DETECTION

Measurements of energetic charged particles from fusion reactions in plasmas are more difficult than for neutrons because one must work within the vacuum system of the plasma container. In this situation a detector is readily exposed to x rays, neutrons, electrons and the ion blow-off from the plasma. A recently developed detection technique which can be used to avoid these problems is a track etch detector.⁸ Certain materials (e.g. cellulose nitrate) are sensitive to the radiation damage of highly ionizing particles such as energetic protons and alpha particles but insensitive to the lesser ionizing radiations from the plasma. Thin films can be exposed to the plasma and then etched in sodium hydroxide to reveal tracks due to radiation damage. These track-etch detectors are particularly suited to plasma experiments and are beginning to be used by more researchers. To cite one example, the group at KMS Fusion has used cellulose nitrate detectors in conjunction with a magnetic spectrograph to determine the α -particle spectrum from the laser implosion of glass shell targets loaded with d-t fuel. The energy loss of the α particles in escaping from the core of the target and their energy spread provide a measure of the temperature and degree of compression in the target implosion.⁹

Pulsed Ion Beams

Some of the more significant developments of nuclear diagnostics for ions have paralleled the increased interest in pulsed ion beams for plasma applications. Such beams are attractive for heating plasmas, for pellet fusion and for producing field-reversing ion rings. In addition interest continues in the development of energetic ions by collective acceleration with intense relativistic electron beam sources. In all of these cases, nuclear techniques have been applied to diagnose such beams. In the remainder of my talk I want to review the developments, which have been summarized in a recent publication.¹⁰

The techniques of nuclear activation have been applied to studies with proton, deuteron and alpha-particle beams. The approach is to measure the gamma-ray activity induced in a target by charged-particle induced nuclear reactions. Target samples are activated by the ion beam, removed and measured with a shielded gamma-ray detector. In this way, the number of incident ions can be determined. Knowledge of the ion energy may be required or inferred from the measurement depending on the particular reaction used.

The following steps are taken to optimize the sensitivity of the activation. First, thick targets are used to optimize the number of reactions. In this case, the reaction yield is given by the integral of the cross section (σ) over the range of the ions in the target. The yield is the number of reactions per incident ion and may be written

$$Y = \int \sigma/\epsilon \, dE$$

where ϵ is the stopping cross section of the target. The stopping cross section is proportional to the stopping power (dE/dx). Second, short-lived activities are used. If a small number of radioactive nuclei (N) are produced, then a short lifetime (τ) is desired to increase the activity ($dN/dt = N/\tau$). However, the lifetime must be long enough to allow the target sample to be removed for counting. Half-lives of the order of minutes are convenient. Third, good detection efficiency with adequate gamma-ray energy resolution is provided by NaI detectors. To achieve low background the detectors may be shielded with a few inches of lead. Also for β^+ activities, coincidence counting with two detectors at 180° to each other is used to reduce the background by several orders-of-magnitude.

For low energy proton beams, (p, γ) resonance reactions are used. The cross section for such a reaction is peaked at the resonance energy, E_R . For a resonance of width Γ , the cross section is given by the resonance expression:

$$\sigma(E) = \frac{\Gamma^2}{4} \frac{\sigma_R}{(E-E_R)^2 + \Gamma^2/4}$$

where σ_R is the cross section at the peak of the resonance. For a resonance with a narrow width, the reaction yield becomes

$$Y_\infty = \pi \sigma_R \Gamma/2\epsilon$$

provided the proton energy is well above the resonance energy, i.e., $E - E_R \gg \Gamma$. The quantity Y_∞ is called the "thick-target step" of a resonance. It is characteristic of a particular nuclear reaction resonance and target composition. If the number of radioactive nuclei produced by a resonance reaction is N_0 , then N_0/Y_∞ is the number of protons with energy greater than the resonance energy.

There are only two (p, γ) reactions on light nuclei which have narrow resonances below 1 MeV and lead to short-lived β^+ activity. The most sensitive is the $^{12}\text{C}(p, \gamma)^{13}\text{N}$ reaction. The thick target yield for this reaction is given in Fig. 7. Two resonances in this reaction at 0.5 and 1.7 MeV are apparent. Between these resonances the yield is nearly constant. It is in this energy region that this reaction is a useful diagnostic.

Estimates of the number of protons that can be detected with the $^{12}\text{C}(p, \gamma)^{13}\text{N}$ reaction as well as with the less sensitive $^{14}\text{N}(p, \gamma)^{15}\text{O}$ reaction are given in Table 2. Here we assume β^+ counting with NaI detectors. The coincidence counting efficiency for 0.51-MeV γ -rays is $\sim 10\%$. The background depends on the environment and shielding. A value of ~ 0.7 cpm is typical. If we count for one mean-life and require at least 10 real counts,

we find the detection limits given in Table 2. In experiments at NRL, these reactions have been used to measure intensities ranging up to 4×10^{16} protons.¹¹

For deuterons of several MeV energy both (d,n) and (d,p) reactions leading to short-lived γ -ray activities can be used to determine the total deuteron number. A list of such reactions is given in Table 3 with the associated γ -ray and half-life. The cross sections for these reactions are small below the Coulomb barrier but increase rapidly as the incident energy is increased. These cross sections do not have narrow resonances, but they do reach values 10^2 to 10^3 times larger than the (p, γ) cross sections, thus increasing the sensitivity. Targets for the reactions in Table 3 are readily available in nearly single isotopic composition, thereby greatly reducing the possibility of interferences from competing reactions.

Thick-target yields for deuterons on carbon and aluminum are given in Fig. 8. In order to determine the deuteron number from an activation measurement, the deuteron energy must be known. Simultaneous activations of both carbon and aluminum can be used to determine mean deuteron energies. The ratio of the yields from C and Al is given in Fig. 8. This ratio is a sensitive function of deuteron energy so that a measured $^{13}\text{N}/^{28}\text{Al}$ ratio can be used to determine the mean deuteron energy. Then the reaction yield at this energy gives the number of deuterons. Two measurements of this ratio for exploded deuterated polyethylene fiber plasmas are shown in Fig. 8. Mean deuteron energies of 5.4 MeV and 7.3 MeV were obtained in these experiments.¹²

More detailed information about the energy distribution of ions may be obtained by activating a stack of thin foils and determining the activation in each foil as a function of the depth into the stack. The depth to which activity is observed provides a measure of the maximum ion energy through the range-energy relation for the ions in the material. In principle the measured activities in a stack of foils can be used to unfold the

incident ion spectrum. However this inversion is difficult in practice because it is sensitive to the differences in activity between adjacent foils and these differences are subject to large errors. Even so, crude energy spectra have been determined in some experiments.¹³

Collective Acceleration

The collective acceleration of positive ions by an intense relativistic electron beam involves the interaction of the ions with strong electrostatic fields associated with the electron beam such that positive ions are accelerated in the same direction that the beam propagates with ion energies substantially larger than the injected electron energy. There is interest in studying this process and its scaling to higher energy because of its potential application to high energy ion acceleration. Ion beams of several MeV energy produced by this process have been measured with threshold reactions, including (p,n) reactions for protons up to 16.5 MeV (Ref. 14) and (α ,xn) reactions where $x = 1,2,3\cdots$ for alpha particles up to 40 MeV (Ref. 15).

The (α ,xn) reactions are threshold reactions which can provide information on both the ion intensity and the energy distribution simultaneously even for a thick target. As an example, cross sections for the $^{181}\text{Ta}(\alpha, xn)^{185-x}\text{Re}$ reactions are shown in Fig. 9. The cross sections at maximum are quite large (~ 1 barn). Since each cross section provides a natural window into the α -particle energy spectrum, thick-target yields can be unfolded to determine the energy spectrum. Each of these reactions produces a radioactive Re nucleus which is a delayed γ -emitter as indicated in Table 4. The γ -ray intensities from different (α ,xn) reactions can be measured simultaneously with a high resolution Ge spectrometer and the number of radioactive nuclei determined. Then α -particle intensities are deduced using the cross sections displayed in Fig. 9.

In summary, the following detection limits are representative of the three different types of ions and energy ranges that I have discussed. For low energy protons, (p, γ) reactions leading to β^+ activity are used and the limit is $\sim 10^{12}$ protons. At higher energies deuteron-induced reactions correspond to a limit of about 10^8 deuterons. A detection limit of $\sim 10^7$ is achieved for 20 to 60 MeV alpha particles by (α ,xn) reactions.

IV. APPENDIX

The application of these nuclear techniques to diverse plasma devices requires a knowledge of how neutrons and ions interact in different materials under various conditions. Much of this type of information is tabulated in specialized references. A list of some sources that may be particularly useful is given below.

1. J.B. Marion and F.C. Young, Nuclear Reaction Analysis, (North-Holland Publ. Co., Amsterdam, 1968).

This is a compilation of properties pertinent to describing the interactions of charged particles, gamma rays and neutrons in various materials.

2. W. Whaling in Handbuch der Physik, ed. E. Flügge, Vol. 34, (Springer-Verlag, Berlin, 1958).

This article on "The Energy Loss of Charged Particles in Matter" gives a review of the experimental status of stopping cross sections and ranges for protons and alpha particles as of 1958.

3. H.H. Anderson and J.F. Ziegler, The Stopping and Ranges of Ions in Matter, (Pergamon Press, New York, 1977).

This is a recent extensive survey of the experimental status of stopping cross sections and ranges for ions in matter. It is arranged in five volumes:

- Vol. 1 The Theory of the Stopping of Ions in Matter
- Vol. 2 Bibliography
- Vol. 3 Hydrogen - Stopping Powers and Ranges
- Vol. 4 Helium - Stopping Powers and Ranges
- Vol. 5 Heavy Ions - Stopping Powers and Ranges

4. Ion Beam Handbook for Material Analysis, eds. J.W. Mayer and E. Rimini, (Academic Press, New York, 1977).

Chapters in this Handbook on "Selected Low Energy Nuclear Reaction Data" and "Energy Loss and Energy Straggling" are relevant to ion diagnostics.

5. C.E. Crouthamel, Applied Gamma-Ray Spectrometry, 2nd. Ed. revised by F. Adams and R. Dams, (Pergamon Press, Oxford, 1970).

The appendices in this book are particularly useful for gamma-ray spectroscopy.

6. M.J. Berger and S.M. Seltzer, Tables of Energy Losses and Ranges of Electrons and Positrons, NASA Report No. SP-3012, 1964.

Available through the National Technical Information Service, Operations Division, Springfield, Virginia, 22151, as Report No. N65-12506.

7. Neutron Cross Sections, BNL 325, 2nd. Ed., Supplement No. 2, Sigma Center, Brookhaven National Laboratory, Vol. 1 (1964), Vol. II (1966), Vol. III (1965).

An extensive compilation of cross sections for neutron interactions for $Z = 1$ to 98 is provided by this group at BNL.

REFERENCES

1. S. Glasstone and R.H. Lovberg, Controlled Thermonuclear Reactions, (D. Van Nostrand Co., Princeton, N.J.) 1960.
2. R.J. Lanter and D.E. Bannerman, "The Silver Counter, A Detector for Bursts of Neutrons," Los Alamos Scientific Laboratory Report LA-3498-MS (July 1966);
R.J. Lanter and D.E. Bannerman, Rev. Sci. Instrum. 39, 1588 (1968).
3. F.C. Young and S.J. Stephanakis, NRL Memo Report 3104 (August 1975).
4. F.C. Young, IEEE Trans. Nucl. Sci. NS-22, 718 (1975).
5. C.E. Spencer and E.L. Jacobs, IEEE Trans. Nucl. Sci. NS-12, 407 (1965); L. Ruby and J.B. Rechen, Nucl. Instrum. Methods 15, 74 (1962) and 53, 60 (1967).
6. L.A. Lerche, L.W. Coleman, J.W. Houghton, D.R. Speck and E.K. Storm, Appl. Phys. Lett. 31, 645 (1977).
7. F.C. Young, D. Mosher, S.J. Stephanakis, S. Goldstein and D. Hinshelwood, NRL Memo Report 3823 (August 1978).
8. R.L. Fleisher, P.B. Price and R.M. Walker, Nuclear Tracks in Solids, (University of California Press, Berkeley, 1975).
9. R. Hofstadter, IEEE Trans. Nucl. Sci. NS-24, 33 (1977).
10. F.C. Young, J. Golden and C.A. Kapetanacos, Rev. Sci. Instrum. 48, 432 (1977).

11. S.J. Stephanakis, D. Mosher, G. Cooperstein, J.R. Boller, J. Golden and S.A. Goldstein, Phys. Rev. Lett. 37, 1543 (1976); J. Golden, C.A. Kapetanakos, S.J. Marsh and S.J. Stephanakis, Phys. Rev. Lett. 38, 130 (1977).
12. F.C. Young, S.J. Stephanakis and D. Mosher, J. Appl. Phys. 48, 3642 (1977).
13. R.B. Miller and D.C. Straw, J. Appl. Phys. 47, 1897 (1976).
14. R.B. Miller and D.C. Straw, IEEE Trans. Nucl. Sci. NS-22, 1022 (1975).
15. S.E. Graybill and F.C. Young, Bull. Am. Phys. Soc. 21, 1058 (1976).
16. J.J. Ramirez and L.W. Kruse, Rev. Sci. Instrum. 47, 832 (1976).

Table 1
Properties of Neutron Activation Detectors

Detector	Geometry	Neutron Energy Sensitivity	Half-life	Counting Time (s)	Bkg (cpm)	Detection Limit at 15 cm (neutrons)	
						2.5 Mev	14 Mev
Ag	6"x6"x12"	All Energies (Moderated)	24 sec 2.3 min	60	200	2 x 10 ⁶	3 x 10 ⁶
Rh	4"diax12"	All Energies (Moderated)	42 sec	60	180	7 x 10 ⁶	2 x 10 ⁷
Pb	7"diax13"	E _n > 1.6 Mev	0.82 sec	2.4	3600	2 x 10 ⁷	1 x 10 ⁸

Table 2

Limits of Detectability for (p, γ) Resonance Reactions

Reaction	Mean-life (min)	Detection Limit (# protons)	Energy Range (MeV)
$^{12}\text{C}(p,\gamma)^{13}\text{N}$	15	2×10^{11}	$0.6 \leq E_p \leq 1.5$
$^{14}\text{N}(p,\gamma)^{15}\text{O}$	3	1×10^{13}	$0.3 \leq E_p \leq 1.0$

Table 3

Properties of Deuteron-Induced Reactions
for Diagnosing Deuterons

Reaction	Natural Isotope Abundance of Target (%)	Half-life of Residual Nucleus (min)	Energy of Delayed γ -ray (MeV)
$^{12}\text{C}(d,n)^{13}\text{N}$	98.89	9.97	0.51
$^{14}\text{N}(d,n)^{15}\text{O}$	99.64	2.04	0.51
$^{27}\text{Al}(d,p)^{28}\text{Al}$	100	2.24	1.78
$^{51}\text{V}(d,p)^{52}\text{V}$	99.75	3.76	1.43

Table 4
 Properties of $^{181}\text{Ta}(\alpha, xn)$ Reactions

Reaction	Half-life	Gamma-ray Energy (keV)	Branching Ratio (γ /decay)
$^{181}\text{Ta}(\alpha, n)^{184}\text{Re}$	38 da.	904	0.40
$^{181}\text{Ta}(\alpha, 2n)^{183}\text{Re}$	71 da.	162	0.23
$^{181}\text{Ta}(\alpha, 3n)^{182}\text{Re}$	64 hr.	1121	0.20
$^{181}\text{Ta}(\alpha, 3n)^{182}\text{Re}$	12.9 hr.	1121	0.38
$^{181}\text{Ta}(\alpha, 4n)^{181}\text{Re}$	19.9 hr.	365	0.65

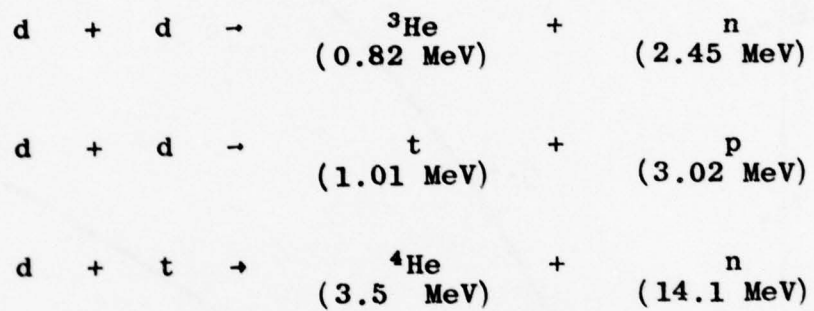


Fig. 1 - Fusion reactions for the hydrogen isotopes. The amount of energy carried off by each particle is indicated. The energy of the incoming particles is assumed to be negligible.

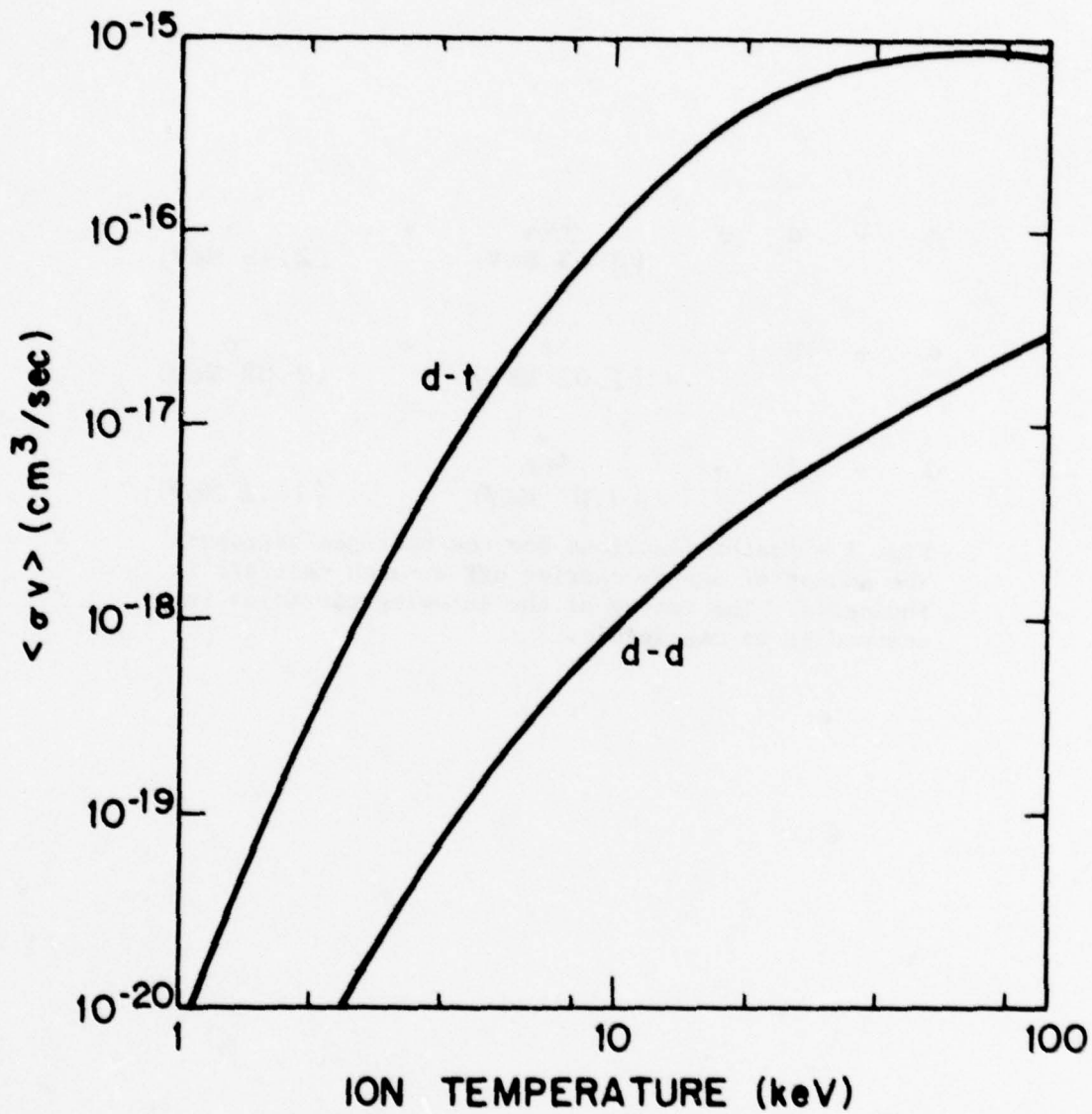


Fig. 2 - The product $\langle \sigma v \rangle$ for the d-t and d-d reactions as a function of ion temperature based on a Maxwellian velocity distribution of the ions.

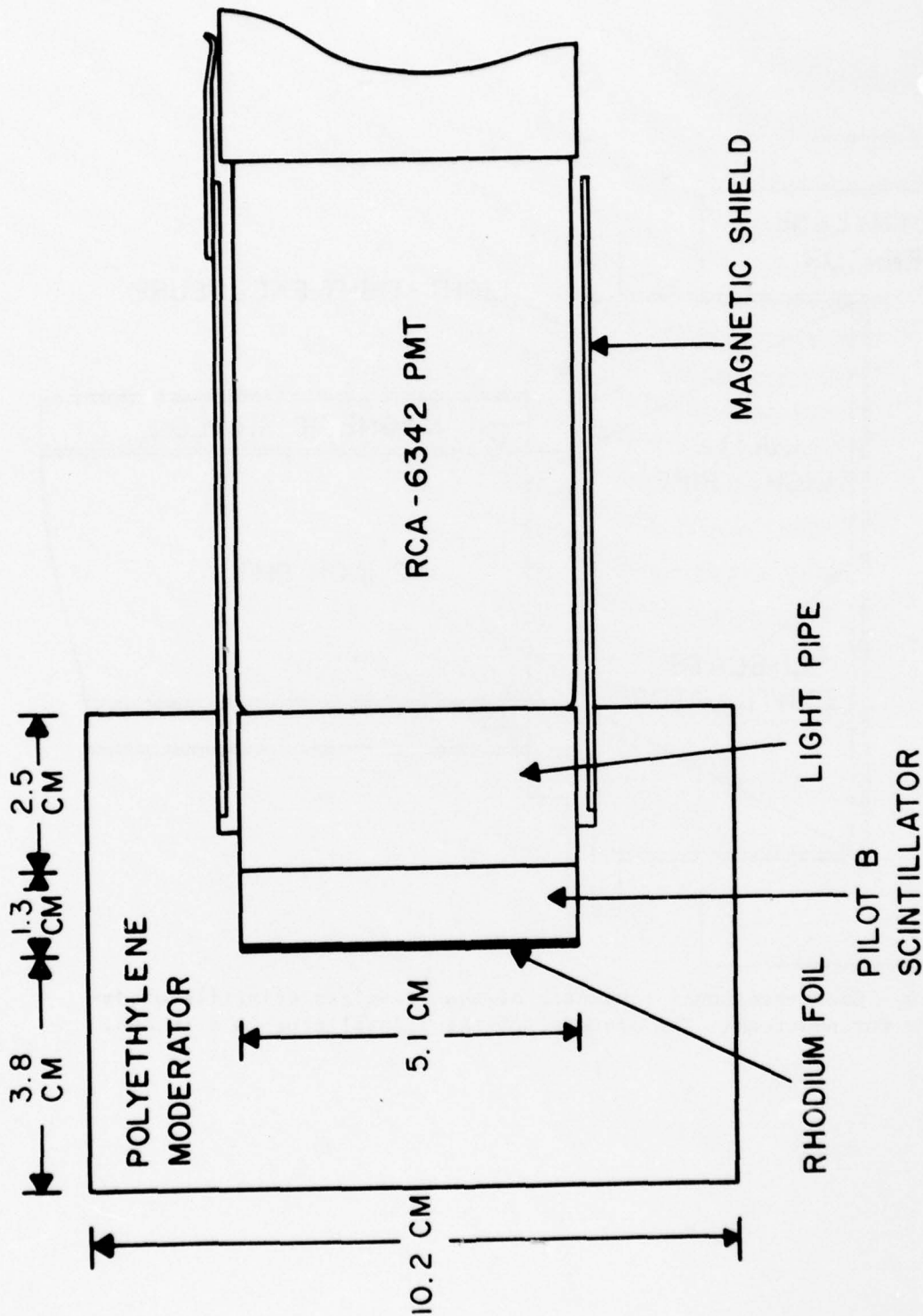


Fig. 3 - Cross-sectional schematic of the Rh-activation detector for neutrons.

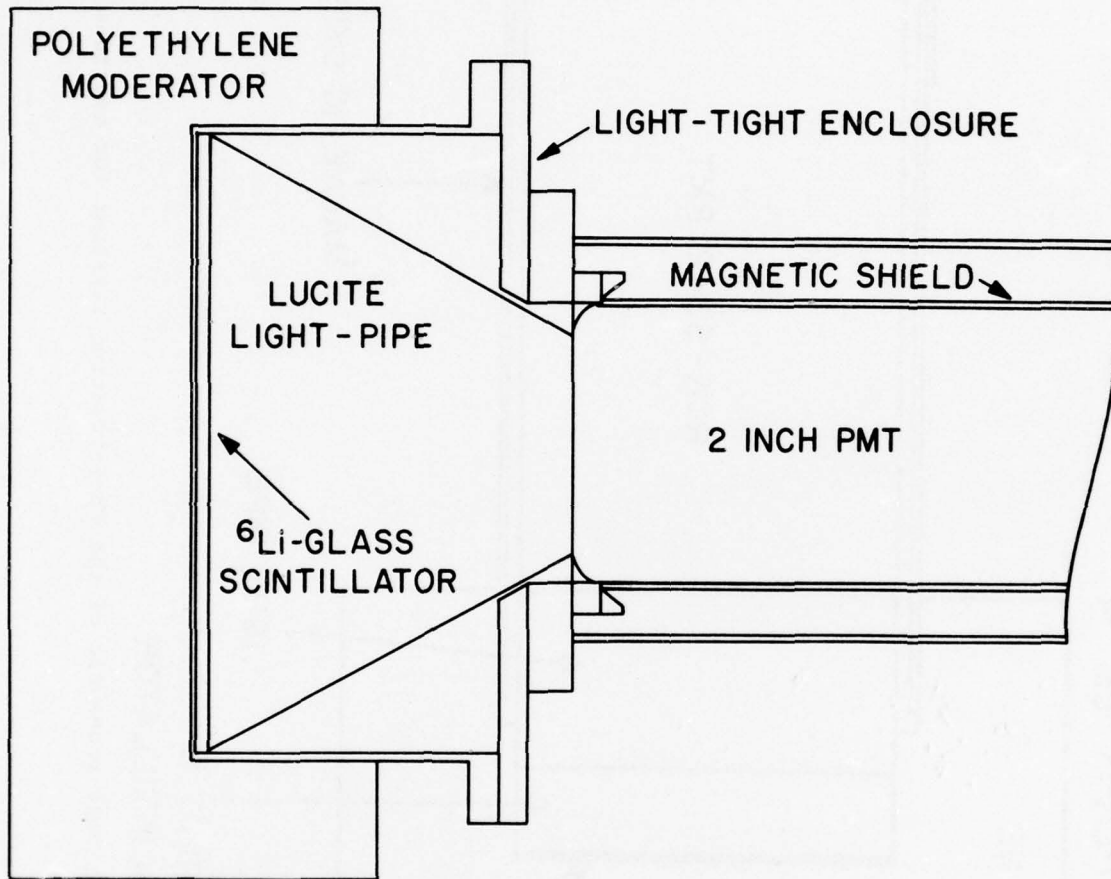


Fig. 4 - Cross-sectional schematic of the ^6Li -glass scintillator detector for neutrons. The diameter of the scintillator is 5 inches.

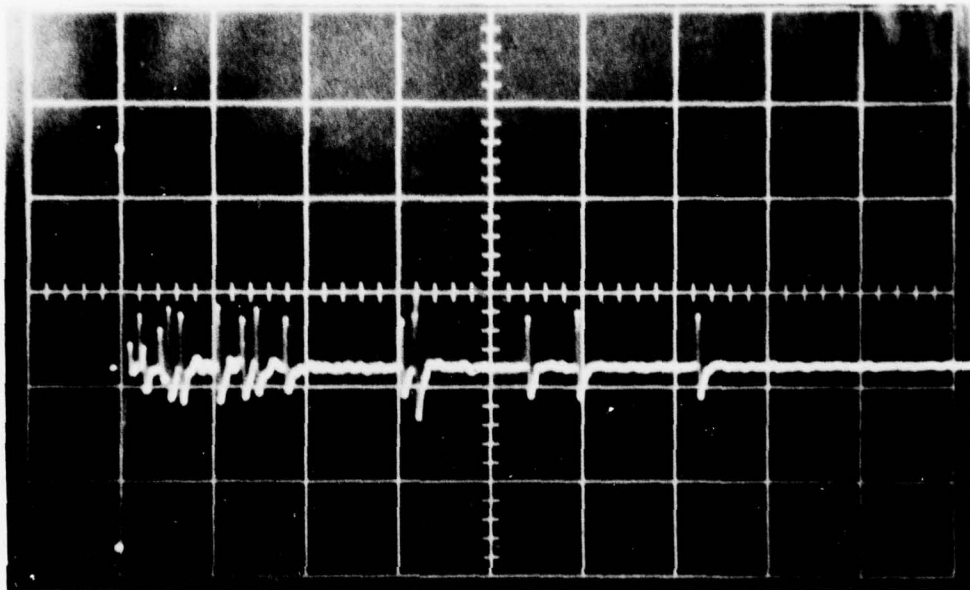


Fig. 5 - Time spectrum of the ${}^6\text{Li}$ -glass detector amplifier output for a single burst of neutrons. The horizontal scale is 50 sec/cm and the vertical scale is 5V/cm.

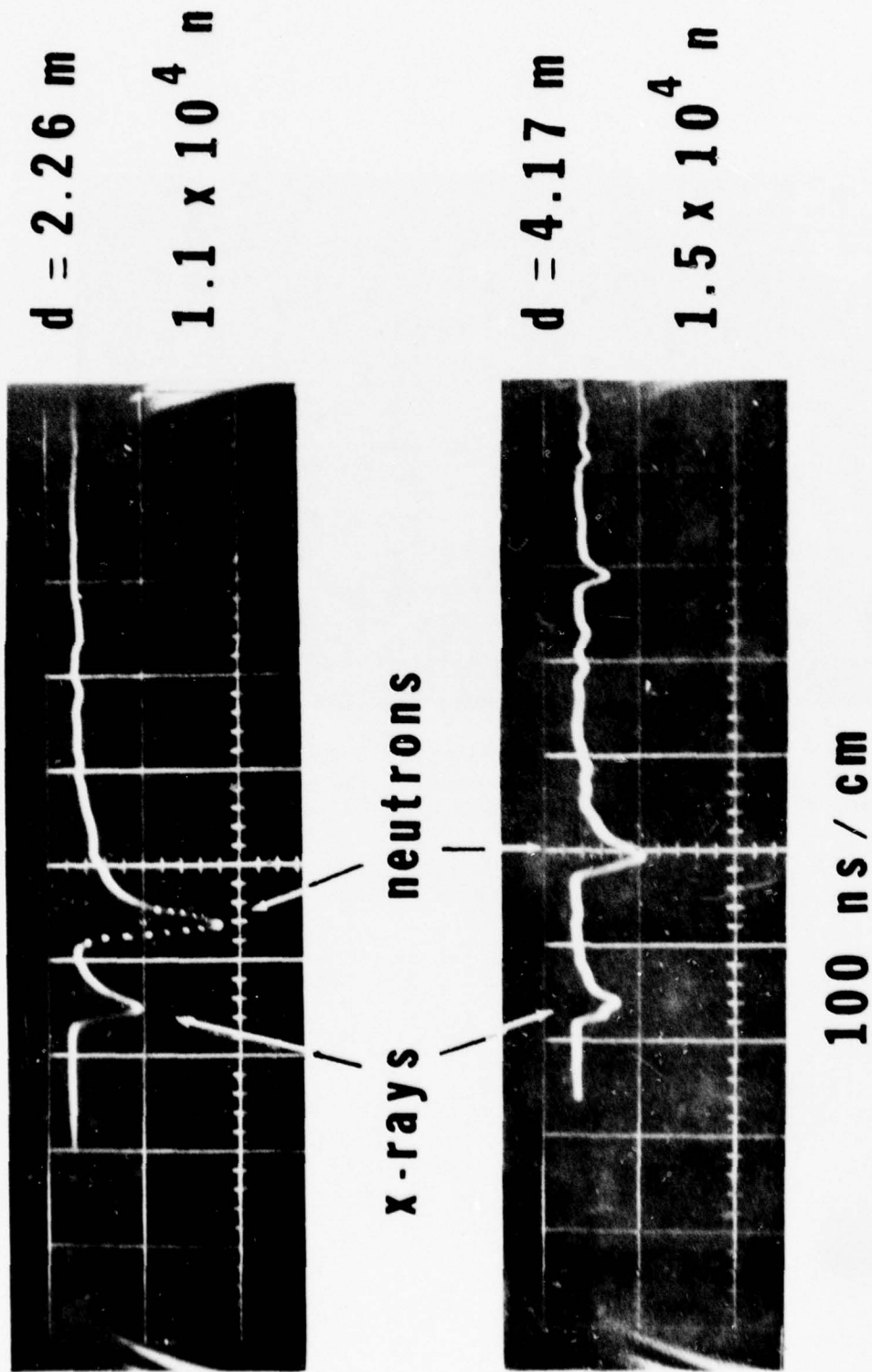


Fig. 6 - Time-of-flight spectra measured on a vacuum spark source. The neutron yields are determined from simultaneous measurements with a ${}^6\text{Li}$ -glass detector.

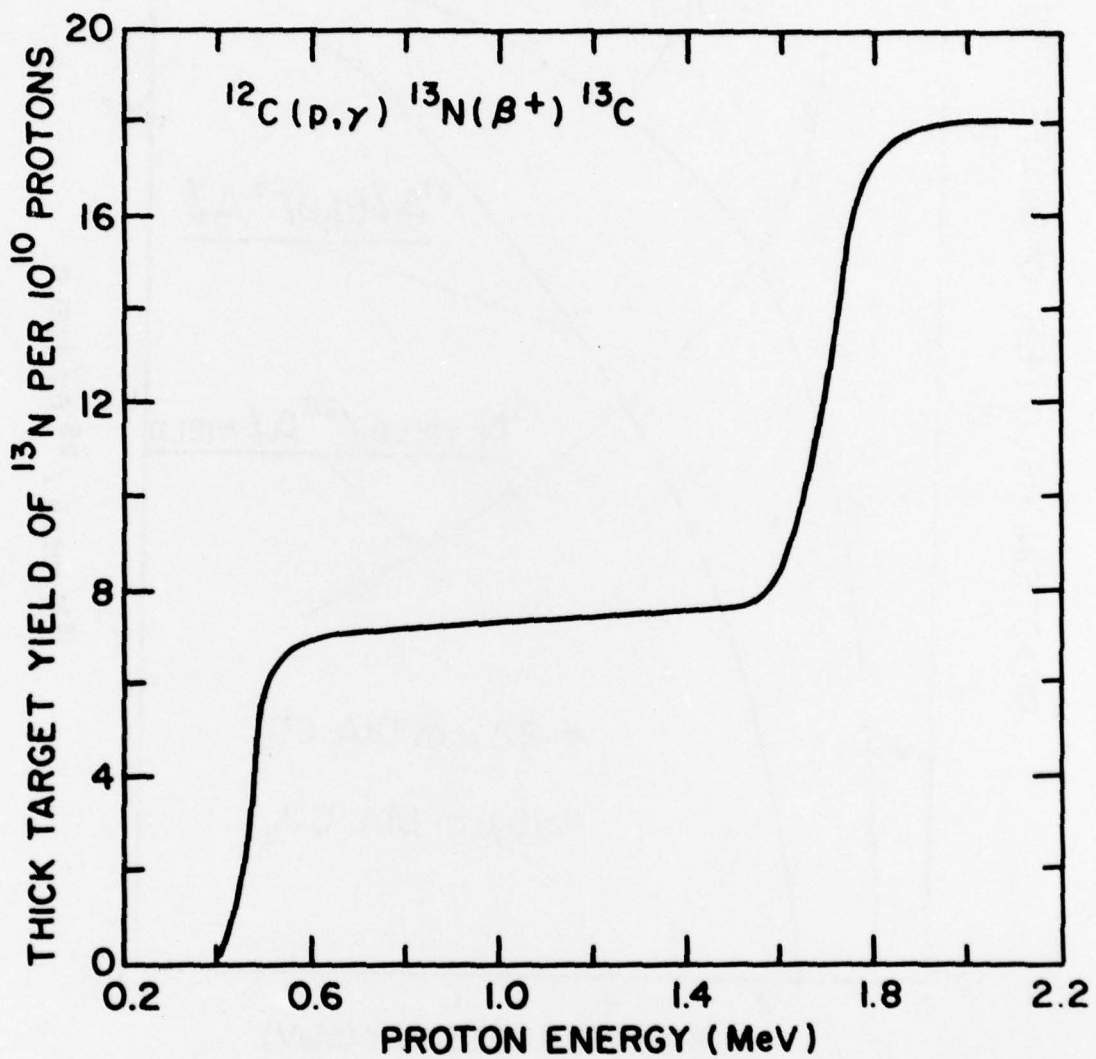


Fig. 7 - Thick-target yield of the $^{12}\text{C}(p,\gamma)^{13}\text{N}(\beta^+)^{13}\text{C}$ reaction.

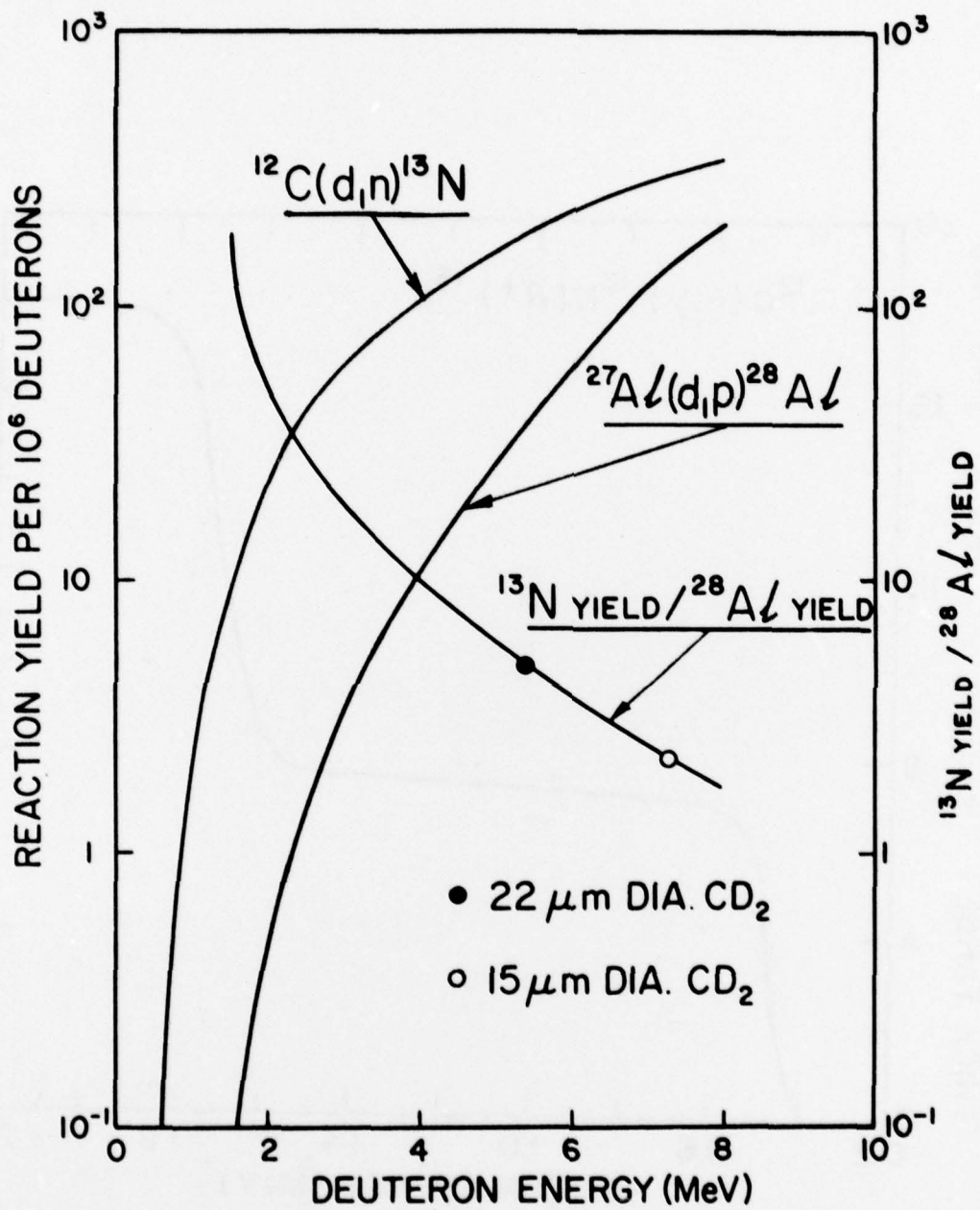


Fig. 8. Thick-target yields for the $^{12}\text{C}(d,n)^{13}\text{N}$ and $^{27}\text{Al}(d,p)^{28}\text{Al}$ reactions and their ratios.

DNA DISTRIBUTION LIST

DEFENSE DOCUMENTATION CENTER
CAMERON STATION
ALEXANDRIA, VA 22314
(12 COPIES IF OPEN PUBLICATION, OTHERWISE 2 COPIES)
12 CY ATTN: TC

DIRECTOR
DEFENSE INTELLIGENCE AGENCY
WASHINGTON, DC 20301
1 CY ATTN: DTICI ROBERT I RUBENSTEIN

DIRECTOR
DEFENSE NUCLEAR AGENCY
WASHINGTON, DC 20305
1 CY ATTN: STVL
1 CY ATTN: TISI ARCHIVES
3 CY ATTN: TITL TECH LIBRARY
1 CY ATTN: RAEV

COMMANDER
FIELD COMMAND
DEFENSE NUCLEAR AGENCY
KIRKLAND AFB, NM 87115
1 CY ATTN: FCPR

DIRECTOR
JOINT STRAT TGT PLANNING STAFF JCS
OFFUTT AFB
OMAHA, NB 68113
1 CY ATTN: JSAS

CHIEF
LIVERMORE DIVISION FLD COMMAND DNA
LAWRENCE LIVERMORE LABORATORY
P.O. BOX 808
LIVERMORE, CA 94550
1 CY ATTN: FCPL

UNDER SEC'Y OF DEF FOR RSCH & ENGRG
DEPARTMENT OF DEFENSE
WASHINGTON, DC 20301
1 CY ATTN: S&SS(OS)

COMMANDER
BMD SYSTEM COMMAND
P.O. BOX 1500
HUNTSVILLE, AL 35807
1 CY ATTN: SSC-TEN

DEP CHIEF OF STAFF FOR RSCH DEV & ACQ
DEPARTMENT OF THE ARMY
WASHINGTON, DC 20310
1 CY ATTN: DAMA-CSM-N

COMMANDER
HARRY DIAMOND LABORATORIES
2800 POWDER MILL ROAD
ADELPHI, MD 20783
(CNWDI-INNER ENVELOPE: ATTN: DELHD-RBH)
1 CY ATTN: DELHD-NP
1 CY ATTN: DELHD-RCC JOHN A. ROSADO
1 CY ATTN: DRXDO-RBH PAUL A. CALDWELL
1 CY ATTN: DRXDO-TI TECH LIB

COMMANDER
PICATINNY ARSENAL
DOVER, NJ 07801
1 CY ATTN: SMUPA ND-N-E

COMMANDER
REDSTONE SCIENTIFIC INFORMATION CTR
U.S. ARMY MISSILE COMMAND
REDSTONE ARSENAL, AL 35809
3 CY ATTN: CHIEF, DOCUMENTS

COMMANDER
U.S. ARMY MISSILE COMMAND
REDSTONE ARSENAL, AL 35809
1 CY ATTN: DRCPM-PE-EA

COMMANDER
U.S. ARMY NUCLEAR AGENCY
7500 BACKLICK ROAD
BUILDING 2073
SPRINGFIELD, VA 22150
1 CY ATTN: ATCN-W

COMMANDER
U.S. ARMY TEST AND EVALUATION COMD
ABERDEEN PROVING GROUND, MD 21005
1 CY ATTN: DRSTE-EL

CHIEF OF NAVAL OPERATIONS
NAVY DEPARTMENT
WASHINGTON, DC 20350

1 CY ATTN: ROBERT A. BLAISE 604C4

COMMANDER
NAVAL ELECTRONIC SYSTEMS COMMAND
NAVAL ELECTRONIC SYSTEMS CMD HQS
WASHINGTON, DC 20360

1 CY ATTN: CODE 5032

COMMANDING OFFICER
NAVAL INTELLIGENCE SUPPORT CTR
4301 SUITLAND ROAD BLDG. 5
WASHINGTON, DC 20390

1 CY ATTN: NISC-45

OFFICER-IN-CHARGE
NAVAL SURFACE WEAPONS CENTER
WHITE OAK, SILVER SPRING, MD 20910

1 CY ATTN: CODE WR43

1 CY ATTN: CODE WA501 NAVY NUC PRGMS OFF

COMMANDER
NAVAL WEAPONS CENTER
CHINA LAKE, CA 93555

1 CY ATTN: CODE 533 TECH LIB

AF WEAPONS LABORATORY, AFSC
KIRTLAND AFB, NM 87117

1 CY ATTN: CA

1 CY ATTN: ELC

1 CY ATTN: NT

1 CY ATTN: SUL

1 CY ATTN: DYP

HQ USAF/RD
WASHINGTON, DC 20330

1 CY ATTN: RDQSM

SAMSO/DY
POST OFFICE BOX 92960
WORLDWAY POSTAL CENTER
LOS ANGELES, CA 90009
(TECHNOLOGY)

1 CY ATTN: DYS

SAMSO/IN
POST OFFICE BOX 92960
WORLDWAY POSTAL CENTER
LOS ANGELES, CA 90009
1 CY ATTN: IND MAJ DARRYL S. MUSKIN

SAMSO/MN
NORTON AFB, CA 92409
(MINUTEMAN)
1 CY ATTN: MNNH

SAMSO/SK
POST OFFICE BOX 92960
WORLDWAY POSTAL CENTER
LOS ANGELES, CA 90009
(SPACE COMM SYSTEMS)
1 CY ATTN: SKF PETER H. STADLER

UNIVERSITY OF CALIFORNIA
LAWRENCE LIVERMORE LABORATORY
P.O. BOX 808
LIVERMORE, CA 94550
1 CY ATTN: L-18
1 CY ATTN: L-153
1 CY ATTN: JOHN NUCKOLLS A DIV L-545 (CLASS L-33)
1 CY ATTN: TECH INFO DEPT L-3

SANDIA LABORATORIES
P.O. BOX 5800
ALBUQUERQUE, NM 87115
1 CY ATTN: DOC CON FOR 3141 SANDIA RPT COLL
1 CY ATTN: DOC CON FOR 5240 GERALD YONAS

AVCO RESEARCH & SYSTEMS GROUP
201 LOWELL STREET
WILMINGTON, MA 01887
1 CY ATTN: RESEARCH LIB A830 RM 7201

BDM CORPORATION THE
7915 JONES BRANCH DRIVE
MCLEAN, VA 22101
1 CY ATTN: TECHNICAL LIBRARY

BOEING COMPANY, THE
P.O. BOX 3707
SEATTLE, WA 98124
1 CY ATTN: AEROSPACE LIBRARY

DIKEWOOD INDUSTRIES, INC.
1009 BRADBURY DRIVE, S.E.
ALBUQUERQUE, NM 87106
1 CY ATTN: L WAYNE DAVIS

EG&G, INC.
ALBUQUERQUE DIVISION
P.O. BOX 10218
ALBUQUERQUE, NM 87114
1 CY ATTN: TECHNICAL LIBRARY

FORD AEROSPACE & COMMUNICATIONS CORP
3939 FABIAN WAY
PALO ALTO, CA 94303
(FORMERLY AERONUTRONIC FORD CORPORATION)
1 CY ATTN: DONALD R. MCMORROW MS G30
1 CY ATTN: LIBRARY

FORD AEROSPACE & COMMUNICATIONS OPERATIONS
FORD & JAMBOREE ROADS
NEWPORT BEACH, CA 92663
(FORMERLY AERONUTRONIC FORD CORPORATION)
1 CY ATTN: TECH INFO SECTION

GENERAL ELECTRIC COMPANY
SPACE DIVISION
VALLEY FORGE SPACE CENTER
GODDARD BLVD KING OF PRUSSIA
P.O. BOX 8555
PHILADELPHIA, PA 19101
1 CY ATTN: JOSEPH C. PEDEN VFSC, RM 4230M

GENERAL ELECTRIC COMPANY
TEMPO-CENTER FOR ADVANCED STUDIES
816 STATE STREET, (P.O. DRAWER QQ)
SANTA BARBARA, CA 93102
1 CY ATTN: DASIAC

INSTITUTE FOR DEFENSE ANALYSES
400 ARMY-NAVY DRIVE
ARLINGTON, VA 22202
1 CY ATTN: IDA LIBRARIAN RUTH S. SMITH

ION PHYSICS CORPORATION
SOUTH BEFORD STREET
BURLINGTON, MA 01803
1 CY ATTN: H. MILDE

IRT CORPORATION
P.O. BOX 81087
SAN DIEGO, CA 92138
1 CY ATTN: R. L. MERTZ

JAYCOR
1401 CAMINO DEL MAR
DEL MAR, CA 92014
1 CY ATTN: ERIC P. WENAAS

JAYCOR
205 S. WHITING STREET, SUITE 500
ALEXANDRIA, VA 22304
1 CY ATTN: ROBERT SULLIVAN

KAMAN SCIENCES CORPORATION
P.O. BOX 7463
COLORADO SPRINGS, CO 80933
1 CY ATTN: ALBERT P. BRIDGES
1 CY ATTN: JOHN R. HOFFMAN
1 CY ATTN: DONALD H. BRYCE
1 CY ATTN: WALTER E. WARE

LOCKHEED MISSILES AND SPACE CO INC
3251 HANOVER STREET
PALO ALTO, CA 94304
1 CY ATTN: LLOYD F. CHASE

MAXWELL LABORATORIES, INC.
9244 BALBOA AVENUE
SAN DIEGO, CA 92123
1 CY ATTN: A. RICHARD MILLER
1 CY ATTN: PETER KORN
1 CY ATTN: ALAN C. KOLB

MCDONNELL DOUGLAS CORPORATION
5301 BOLSA AVENUE
HUNTINGTON BEACH, CA 92647
1 CY ATTN: STANLEY SCHNEIDER

MISSION RESEARCH CORPORATION
735 STATE STREET
SANTA BARBARA, CA 93101
1 CY ATTN: WILLIAM C. HART
1 CY ATTN: CONRAD L. LONGMIRE

MISSION RESEARCH CORPORATION-SAN DIEGO
P.O. BOX 1209
LA JOLLA, CA 92038
(VICTOR A. J. VAN LINT)
1 CY ATTN: V. A. J. VAN LINT

NORTHROP CORPORATION
NORTHROP RESEARCH AND TECHNOLOGY CTR
3401 WEST BROADWAY
HAWTHORNE, CA 90250
(DESIRES ONLY 1 COPY OF CNWDI MAT)
1 CY ATTN: LIBRARY

NORTHROP CORPORATION
ELECTRONIC DIVISION
2301 WEST 120TH STREET
HAWTHORNE, CA 90250
1 CY ATTN: VINCENT R. DEMARTINO

PHYSICS INTERNATIONAL COMPANY
2700 MERCED STREET
SAN LEANDRO, CA 94577
1 CY ATTN: DOC CON FOR BERNARD H. BERNSTEIN
1 CY ATTN: DOC CON FOR CHARLES H. STALLINGS
1 CY ATTN: DOC CON FOR PHILIP W. SPENCE
1 CY ATTN: DOC CON FOR IAN D. SMITH
1 CY ATTN: DOC CON FOR SIDNEY D. PUTNAM

PULSAR ASSOCIATES, INC.
11491 SORRENTO VALLEY BLVD
SAN DIEGO, CA 92121
1 CY ATTN: CARLETON H. JONES JR.

R & D ASSOCIATES
P.O. BOX 9695
MARINA DEL REY, CA 90291
1 CY ATTN: C. MACDONALD
1 CY ATTN: WILLIAM R. GRAHAM JR.
1 CY ATTN: LEONARD SCHLESSINGER

SCIENCE APPLICATIONS, INC.
P.O. BOX 2351
LA JOLLA, CA 92038
1 CY ATTN: J. ROBERT BEYSTER

SPIRE CORPORATION
P.O. BOX D
BEDFORD, MA 01730
1 CY ATTN: ROGER G. LITTLE

SRI INTERNATIONAL
333 RAVENSWOOD AVENUE
MENLO PARK, CA 94025
1 CY ATTN: SETSUO DDAIRIKI

SYSTEMS, SCIENCE AND SOFTWARE, INC.
P.O. BOX 4803
HAYWARD, CA 94540
1 CY ATTN: DAVID A. MESKAN

SYSTEMS, SCIENCE AND SOFTWARE, INC.
P.O. BOX 1620
LA JOLLA, CA 92038
1 CY ATTN: ANDREW R. WILSON

TEXAS TECH UNIVERSITY
P.O. BOX 5404 NORTH COLLEGE STATION
LUBBOCK, TX 79417
1 CY ATTN: TRAVIS L. SIMPSON

TRW DEFENSE & SPACE SYS GROUP
ONE SPACE PARK
REDONDO BEACH, CA 90278
1 CY ATTN: TECH INFO CENTER/S-1930

VOUGHT CORPORATION
MICHIGAN DIVISION
38111 VAN DYKE ROAD
STERLING HEIGHTS, MI 48077
(FORMERLY LTV AEROSPACE CORPORATION)
1 CY ATTN: TECH LIB

NRL CODE 2628 - 20 CYS

NRL CODE 6700 - 1 CY

NRL CODE 6770 - 20 CYS (1 CY CLASSIFIED)

DOE DISTRIBUTION LIST

1. U. S. Department of Energy
Washington, D.C. 20545
Attn: Dr. Leslie S. Levine
Dr. David F. Sutter
Dr. William A. Wallenmeyer
Dr. Daniel R. Miller
Dr. Terry F. Godlove

2. Lawrence Livermore Laboratory
P. O. Box 808
Livermore, Calif. 94550
Attn: Dr. John L. Emmett
Dr. James A. Maniscalco
Dr. Richard J. Briggs

Dr. Roger O. Bangerter
Dr. Donald J. Meeker

3. KMS Fusion, Inc.
3941 Research Park Drive
P. O. Box 1567
Ann Arbor, Michigan 48106
Attn: Dr. Henry J. Gomberg

4. University of Rochester
Laboratory for Laser Energetics
River Station, Hopeman 110
Rochester, New York 14627
Attn: Dr. Moshe J. Lubin

5. Sandia Laboratories
P. O. Box 5800
Albuquerque, New Mexico 87115
Attn: Dr. Everet H. Beckner
Dr. Glenn W. Kuswa (Org. 5244)
Dr. Milton J. Clauser

Dr. Alan J. Toepfer (Org. 5242)
Dr. John R. Freeman (Org. 5241)

6. University of Maryland
Inst. for Fluid Dynamics and
Res. Mathematics
College Park, Md. 20742
Attn: Dr. Derek A. Tidman

7. University of California
Lawrence Berkeley Laboratory
Berkeley, Calif. 94720
Attn: Dr. Edward J. Lofgren
Dr. Denis Keefe
8. National Bureau of Standards
Washington, D.C. 20234
Attn: Dr. James Leiss
9. Los Alamos Scientific Laboratory
P. O. Box 1663
Los Alamos, New Mexico 87545
Attn: Dr. Roger B. Perkins
10. Cornell University
Ithaca, New York 14850
Attn: Dr. Ravi N. Sudan
Dr. David A. Hammer
11. Stanford University
Stanford Linear Accelerator Center
P. O. Box 4349
Stanford, Calif. 94305
Attn: Dr. William B. Herrmannsfeldt
12. National Science Foundation
Mail Stop 19
Washington, D.C. 20550
Attn: Dr. David Berley
13. Argonne National Laboratory
9700 South Cass Avenue
Argonne, Illinois 60439
Attn: Dr. Ronald L. Martin
Dr. Thomas H. Fields
14. Director
Defense Nuclear Agency
Washington, D.C. 20305
Attn: Dr. H. Carl Fitz, Jr. (RAEV)
Mr. Jonathon Z. Farber (RAEV)
MAJ Howard W. Kympton (RAEV)
15. Maxwell Laboratories, Inc.
9244 Balboa Avenue
San Diego, Calif. 92123
Attn: Dr. A. W. Trivelpiece
Dr. Peter Korn
Dr. Allen C. Kolb

16. Brookhaven National Laboratory
Upton, New York 11973
Attn: Dr. Alfred F. Maschke

DEPARTMENT OF THE NAVY

NAVAL RESEARCH LABORATORY
Washington, D. C. 20375

OFFICIAL BUSINESS

PENALTY FOR PRIVATE USE, \$300

POSTAGE AND FEES PAID
DEPARTMENT OF THE NAVY
DOD-316
THIRD CLASS MAIL

